Textile-Reinforced Mortar versus FRP Jacketing in Seismic Retrofitting of RC Columns with Continuous or Lap-Spliced Deformed Bars

D. A. Bournas[1]; T. C. Triantafillou, M.ASCE[2]; K. Zygouris[3]; and F. Stavropoulos[4]

Abstract: The effectiveness of a new structural material, namely, textile-reinforced mortar (TRM), was investigated experimentally in this study as a means of confining oldtype reinforced concrete (RC) columns with limited capacity due to bar buckling or due to bond failure at lap splice regions. Comparisons with equal stiffness and strength fiber-reinforced polymer (FRP) jackets allow for the evaluation of the effectiveness of TRM versus FRP. Tests were carried out on nearly full scale nonseismically detailed RC columns subjected to cyclic uniaxial flexure under constant axial load. Ten cantilevertype specimens with either continuous or lap-spliced deformed longitudinal reinforcement at the floor level were constructed and tested. Experimental results indicated that TRM jacketing is quite effective as a means of increasing the cyclic deformation capacity of oldtype RC columns with poor detailing, by delaying bar buckling and by preventing splitting bond failures in columns with lap-spliced bars. Compared with their FRP counterparts, the TRM jackets used in this study were found to be equally effective in terms of increasing both the strength and deformation capacity of the retrofitted columns. From the response of specimens tested in this study, it can be concluded that TRM jacketing is an extremely promising solution for the confinement of reinforced concrete columns, including poorly detailed ones with or without lap splices in seismic regions.

DOI: 10.1061/(ASCE)CC.1943-5614.0000028

CE Database subject headings: Buckling; Confinement; Reinforced concrete; Concrete columns; Seismic effects; Rehabilitation; Mortars.

Introduction and Background

The upgrading of existing reinforced concrete (RC) structures through jacketing of columns has become a very popular technique in an increasingly large number of rehabilitation projects, both seismic and nonseismic. The use of fiber-reinforced polymers (FRPs) has gained considerable popularity among all jacketing techniques, due to the favorable properties offered by these materials, namely, high strength to weight ratio, corrosion resistance, ease and speed of application, and minimal change of geometry. Despite all these advantages, the FRP retrofitting technique has a few drawbacks, e.g., poor behavior at high temperatures, high costs, inapplicability on wet surfaces or at low temperatures, hazards for the manual worker—even though modern epoxies gradually become less hazardous due to smaller solvent contents, lack of vapor permeability—which may cause damage to the concrete structure, and difficulty to conduct postearthquake assessment behind FRP jackets. These are mainly attributed to the organic epoxy resins used to bind the fibers. An interesting alternative to FRP materials are the so-called textile-reinforced mortars (TRMs) (Triantafillou et al. 2006). These new materials are made of textiles, that are fabric meshes made of long woven, knitted or even unwoven fiber rovings in at least two directions, impregnated with inorganic binders, such as cement-based mortars. The density, that is the quantity and the spacing, of rovings in each direction can be controlled independently, thus affecting the mechanical characteristics of the textile and the degree of penetration of the mortar matrix through the mesh.

Studies on the use of textiles as reinforcing materials of cement-based products commenced in the early 1980s, but developments in this field progressed slowly until the late 1990s. However, during the past few years the research community has put substantial effort on the use of textiles as reinforcement of cementitious products, mainly in new constructions (e.g., Curbach and Jesse 1999; Brameshuber et al. 2001; Hegger and Voss 2007). Research on the use of textiles in the upgrading of concrete structures has been limited. Most of the studies concern the bond between concrete and cement-based textile composites, as well as flexural or shear strengthening of beams (Curbach and Ortlepp 2003; Brueckner et al. 2005; Triantafillou and Papanicolaou 2006). In these studies it was concluded that properly designed textiles combined with cement-based binders have a good potential as strengthening materials of RC members. The first study reported in the literature on the use of textiles in combination with cementitious binders for the confinement of concrete is that of Triantafillou et al. (2006). In this study the writers investigated experimentally the application of TRM as a means of increasing the axial strength of plain concrete through confinement and they compared the behavior of TRM-confined cylinders and prisms

[1]Formerly, Ph.D. Student, Dept. of Civil Engineering, Univ. of Patras, Patras GR-26500, Greece. E-mail: dbournas@upatras.gr

[2]Professor, Dept. of Civil Engineering, Univ. of Patras, Patras GR-26500, Greece (corresponding author). E-mail: ttriant@upatras.gr

[3]Formerly, Graduate Student, Dept. of Civil Engineering, Univ. of Patras, Patras GR-26500, Greece. E-mail: kzygouris@upatras.gr

[4]Formerly, Graduate Student, Dept. of Civil Engineering, Univ. of Patras, Patras GR-26500, Greece. E-mail: fstavr@upatras.gr

Note. This manuscript was submitted on July 31, 2008; approved on February 23, 2009; published online on March 6, 2009. Discussion period open until March 1, 2010; separate discussions must be submitted for individual papers. This paper is part of the ***Journal of Composites for Construction***, Vol. 13, No. 5, October 1, 2009. ©ASCE, ISSN 1090-0268/2009/5-360–371/$25.00.

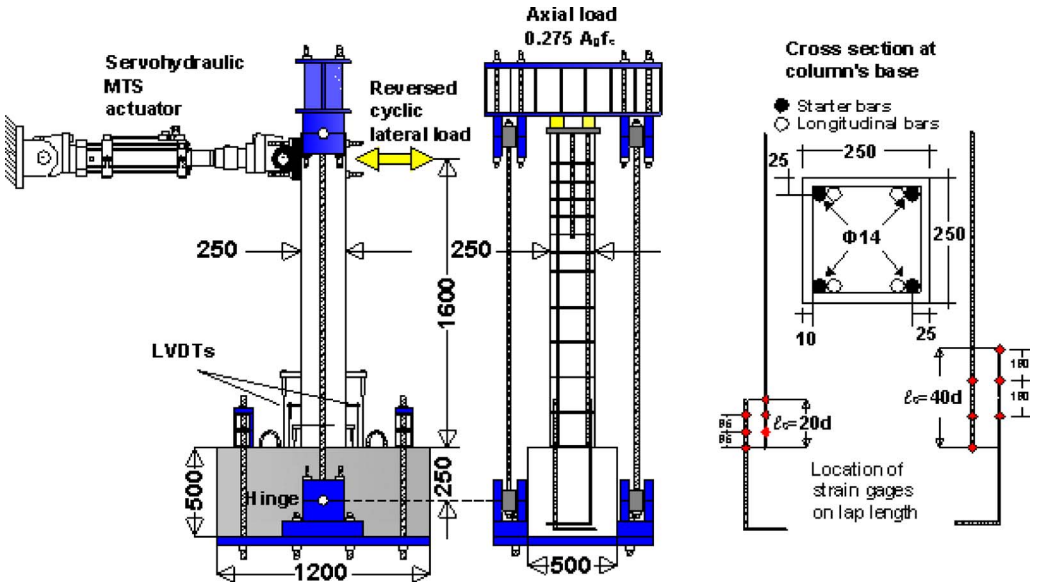

Fig. 1. (a) Schematic of test setup; (b) cross section of the columns and distribution of strain gauges along the lap length

with that of specimens confined with FRP jackets of equal stiffness and strength. Main conclusions were that: (a) TRM jacketing provides a substantial increase in compressive strength and deformation capacity of plain concrete; and (b) compared with their FRP counterparts, TRM jackets may result in slightly reduced effectiveness.

In a more recent study, Bournas et al. (2007) investigated experimentally the use of TRM jackets as a means of confining poorly detailed RC columns, which suffer from limited deformation capacity under seismic loads due to buckling of the longitudinal bars. Tests were carried out both on short prisms under concentric compression, reproducing the behavior of compression zones in RC members where bar buckling is critical, and on nearly full scale nonseismically detailed RC columns with smooth bars subjected to cyclic uniaxial flexure under constant axial load. All specimens retrofitted with TRM jackets had their FRP-retrofitted counterpart, which enabled comparisons of the two systems. Main conclusion in this study was that TRM jacketing is quite effective (and equally to its FRP counterpart) as a means of increasing the cyclic deformation capacity and the energy dissipation of oldtype RC columns with poor detailing, by delaying bar buckling.

In the present study the writers go one step further by investigating experimentally the use of TRM jackets as a means of confining poorly detailed oldtype RC columns with deformed rebars, which suffer from limited deformation capacity under seismic loads due to either buckling of the longitudinal bars or bond failure at lap splice regions.

Experimental Program

Test Specimens and Experimental Parameters

A total of 10 large scale reinforced concrete column specimens with the same geometry were constructed and tested under cyclic uniaxial flexure with constant axial load [Fig. 1(a)]. Four of the columns were reinforced with continuous longitudinal reinforcement and six columns had lap-spliced rebars at the base. The specimens were flexure-dominated cantilevers with a height to the point of application of the load (shear span) of 1.6 m (half a typical story height) and a cross section of 250×250 mm^2. The columns were fixed into a heavily reinforced 0.5-m-deep base block, 1.2×0.5 m^2 in plan, within which the longitudinal bars were anchored with 90º hooks at the bottom. To represent oldtype nonseismically designed and detailed columns, both series of continuous and spliced specimens were reinforced longitudinally with four 14-mm-diameter deformed bars with an effective depth of 225 mm and 8-mm diameter smooth stirrups at a spacing of 200 mm, closed with 90º hooks at both ends. The geometry of a typical cross section is shown in Fig. 1(b).

Four specimens were constructed with continuous longitudinal reinforcement (Series L0_…). One specimen was tested without retrofitting, as control (L0_C), the second one was retrofitted with a double-layered carbon fiber-reinforced polymer (CFRP) jacket (Specimen L0_R2), the third one was retrofitted with an equal (to its FRP counterpart) stiffness and strength carbon fiber TRM jacket comprising four layers (Specimen L0_M4), and the last specimen was retrofitted with a lower stiffness and strength four-layered glass fiber TRM jacket (Specimen L0_M4G), which represents a rehabilitation solution of lower cost in comparison with specimen L0_R2 and L0_M4 in practical strengthening applications.

The effectiveness of TRM versus FRP jackets, applied at the ends of oldtype RC columns for specimens constructed with lap splicing of longitudinal reinforcement above the column base, was evaluated for two different lap lengths, which were selected equal to 20 and 40 bar diameters, as shown in Fig. 1(b). Columns with the shorter lap lengths (Series L20d_…) are more representative of RC construction up to the late 1970s. These columns were designed as follows: one specimen was tested without retrofitting as control (L20d_C), the second one was retrofitted with a two-layered CFRP jacket (specimen L20d_R2) and the third one was retrofitted with an equal (to its FRP counterpart) stiffness and strength carbon fiber TRM jacket comprising four layers (Specimen L20d_M4). Columns with longer lap lengths (Series L040d_…) are more representative of RC construction up to the

Table 1. Experimental Parameters

Specimen notation	Lap length	Concrete strength f_c (MPa)	Confinement with composite materials		
			Jacketing materials	Fibers	Number of layers/ jacket's height
L0_C	—	28.9	—	—	—
L0_R2	—	28.6	FRP	Carbon	2/430 mm
L0_M4	—	28.4	TRM	Carbon	4/430 mm
L0_M4G	—	28.3	TRM	Glass	4/430 mm
L20d_C	$20d_b$=280 mm	27.8	—	—	—
L20d_R2	$20d_b$=280 mm	26.5	FRP	Carbon	2/430 mm
L20d_M4	$20d_b$=280 mm	26.3	TRM	Carbon	4/430 mm
L40d_C	$40d_b$=560 mm	25.8	—	—	—
L40d_R2	$40d_b$=560 mm	25.5	FRP	Carbon	2/600 mm
L40d_M4	$40d_b$=560 mm	25.3	TRM	Carbon	4/600 mm

late 1990s. These columns were given the notation L40d_C, L40d_R2, and L40d_M4, that is identical to Series L20d_…, except for the lap length.

Note that the layers in the TRM-jacketed columns were twice as many compared with their FRP counterparts, resulting in two "equivalent" confining systems, that is with equal stiffness and strength in the circumferential direction (as explained below, the fibers of the two jacketing systems in the circumferential direction were of the same type and nearly twice as many in the FRP system compared with the TRM system).

In summary, the notation of specimens is L*X*_Y*N*, where *X* defines the lap splice length above the column base (0 for continuous reinforcement, 20d for a lap splice length of 20 rebar diameters, 40d for a lap splice length of 40 rebar diameters), Y denotes the type of jacket (C for the unjacketed—control columns, R for resin-based jackets, and M for mortar-based jackets) and *N* denotes the number of layers. For the specimen strengthened with a glass fiber TRM jacket the letter G was added after letter *N*.

The jackets extended from the base of each column (a gap of about 10 mm was left) to a height of 430 mm except for the two columns with longer lap splices (L40d_R2 and L40d_M4) where the jackets were extended to a height of 600 mm. The overlapping length of the jacket was equal to 150 mm. Prior to jacketing, the four corners of the columns which received jacketing were rounded at a radius equal to 25 mm. A summary of the experimental parameters and retrofitting schemes is presented in Table 1.

Materials and Strengthening Procedures

The longitudinal bars had a yield stress of 523 MPa, a tensile strength of 624 MPa, and an ultimate strain equal to 12% (average values from six specimens). The corresponding values for the steel used for stirrups were 351 MPa, 444 MPa, and 19.5%. To simulate field conditions the base blocks and the columns were cast with separate batches of ready-mix concrete (on two consecutive days). Casting of the columns was made with separate batches too, due to the unavailability of a large number of molds. The compressive strengths on the day of testing the columns, measured on $150\times150\times150$ mm^3 cubes (average values from three specimens), are presented in Table 1 for all columns. The average compressive strength and standard deviation were equal to 27.14 and 1.40 MPa, respectively, suggesting that the variability in concrete strength would not affect much the column test results. Cylinders with a diameter of 150 mm and a height of 300 mm were also used to obtain the splitting tensile strength of the concrete; the average tensile strength which was obtained from six specimens on the day of testing the columns was equal to 3 MPa.

For the specimens receiving TRM jacketing (L0_M4, L0_M4_G, L20d_M4, and L40d_M4) two commercial textiles with equal quantity of carbon or glass rovings in two orthogonal directions were used [Fig. 2(a)]. Each fiber roving was 3-mm wide and the clear spacing between rovings was 7 mm. The weight of carbon and glass fibers in the textiles was 348 and 480 g/m^2, respectively, while the nominal thickness of each layer (based on the equivalent smeared distribution of fibers) was 0.095 and 0.089 mm, respectively. The mean tensile strength of the carbon and glass fibers (as well as of the textiles, when the nominal thickness is used) was taken from data sheets equal to 3,800 and 1,700 MPa, respectively. The elastic modulus of carbon and glass fibers was 225 and 70 GPa, respectively. For the specimens receiving FRP jacketing (L0_R2, L20d_R2, and L40d_R2), a commercial unidirectional carbon fiber sheet was used, with a weight of 300 g/m^2 and a nominal thickness of 0.17 mm. For the specimens receiving mortar as a binding material, a commercial inorganic dry binder was used, consisting of cement and polymers at a ratio of about 8:1 by weight. The water:binder ratio in the mortar was 0.23:1 by weight, resulting in plastic consistency and good workability. Finally, for the specimens receiving resin adhesive bonding, a commercial structural adhesive (two-part epoxy resin with a mixing ratio 3:1 by weight) was used with a tensile

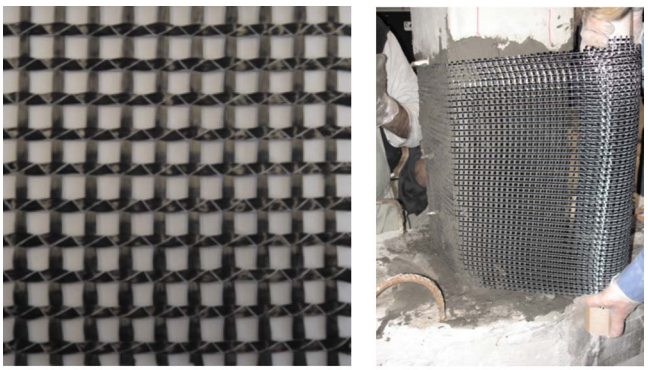

Fig. 2. (a) Photograph of textile used in this study; (b) application of TRM jacket

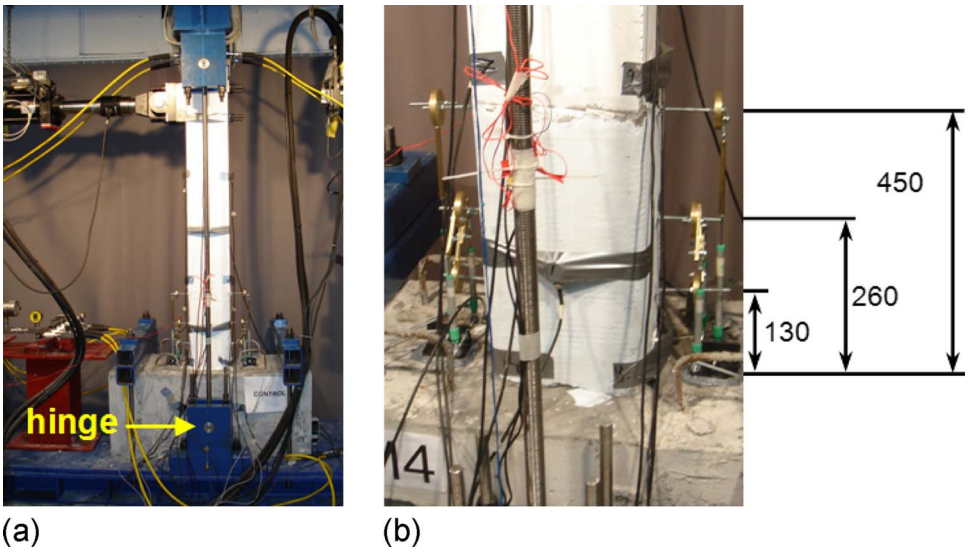

Fig. 3. (a) Photograph of test setup; (b) position of displacement transducers (dimensions in millimeter)

strength of 70 MPa and an elastic modulus of 3.2 GPa (cured for 7 days at 23°C). The adhesive had low viscosity such that complete wetting of the sheets was possible by using a plastic roller.

Application of the mortar was made in approximately 2-mm-thick layers with a smooth metal trowel. After application of the first mortar layer on the (dampened) concrete surface, the textile was applied and pressed slightly into the mortar, which protruded through all the perforations between fiber rovings. The next mortar layer covered the textile completely and the operation was repeated until all textile layers were applied and covered by the mortar. Of crucial importance in this method, as in the case of epoxy resins, was the application of each mortar layer while the previous one was still in a fresh state. A photograph of the application method of textile combined with mortar binder to provide jacketing in one of the specimens used in this study is shown in Fig. 2(b).

The strength of mortar used in this study was obtained through flexural and compression testing according to EN 1015-11 (European Committee for Standardization 1993), using a servohydraulic MTS testing machine. Flexural testing was carried out on three $40\times40\times160$ mm^3 hardened mortar prisms, at an age of 28 days. The prisms were prepared and cured in the laboratory until testing, in conditions identical to those for the jackets used for confinement (except for the first 2 days, when the prisms were inside the molds). The prisms were subjected to three-point bending at a span of 100 mm and from the peak load the flexural strength was calculated. Compression testing was carried out on each of the fractured parts using two 40×40 mm^2 bearing steel platens on top and bottom of each specimen. The average flexural and compressive strength values were 6.51 and 20.8 MPa, respectively.

Experimental Setup and Procedure

To simulate seismic excitation, the columns were subjected to lateral cyclic loading which consisted of successive cycles progressively increasing by 5 mm of displacement amplitudes in each direction. The loading rate was in the range from 0.2 to 1.1 mm/s, the higher rate corresponding to higher displacement amplitude, all in displacement-control mode. At the same time a constant axial compressive load was applied to the columns, corresponding to 27.5% of the members' compressive strength (depending on concrete strength, this load ranged from 435 to 496 kN). The lateral load was applied using a horizontally positioned 250-kN MTS actuator and the axial load was exerted by a set of four hydraulic cylinders with automated pressure self-adjustment, acting against two vertical rods connected to the strong floor of the testing frame through a hinge [Figs. 1(a) and 3(a). With this setup the $P-\Delta$ moment at the base section of the column is equal to the axial load times the tip displacement (that is at piston fixing position) of the column, times the ratio of hinge distance from the base (0.25 m) and the top ($0.25+1.60=1.85$ m) of the column (that is times $0.25/1.85=0.135$).

Displacements, rotations, and curvatures at the plastic hinge region were monitored using six rectilinear displacement transducers (three on each side, perpendicular to the piston axis) fixed at cross sections 1, 2, and 3, with a distance equal to $\ell_1=130$ mm, $\ell_2=260$ mm, and $\ell_3=450$ mm, respectively, from the column base, as shown in Fig. 3(b). The instrumentation also comprised a total of eight strain gauges for each column with continuous longitudinal reinforcement and a total of 12 strain gauges for each column with lap splices. For the columns with continuous bars two strain gauges were mounted on each reinforcing bar (at a height of 100 mm from the base cross section) to estimate the strain of longitudinal bars at the onset of buckling. This location was chosen as buckling is expected to occur at the midheight between the first two stirrups above the column base. The 12 strain gauges of the columns with lap splices were mounted on one pair of lapped bars (starter-longitudinal) per column side as follows [Fig. 1(b)]: (a) three along the starter bars at distances from the column base equal to 0, 95, and 190 mm (for Series L20d_…), or 0, 195, and 390 mm (for Series L40d_…); and (b) three along the longitudinal bars at distances from the column base equal to 95, 190, and 280 mm (for Series L20d_…), or 195, 390, and 560 mm (for Series L40d_…). Measurements from the strain gauges on each pair of starter-longitudinal bars were used to determine the strain distribution of bars and bond stresses along the splice length.

Test Results and Discussion

The response of all columns tested is given in Fig. 4 in the form of load-drift ratio (obtained by dividing the tip displacement with

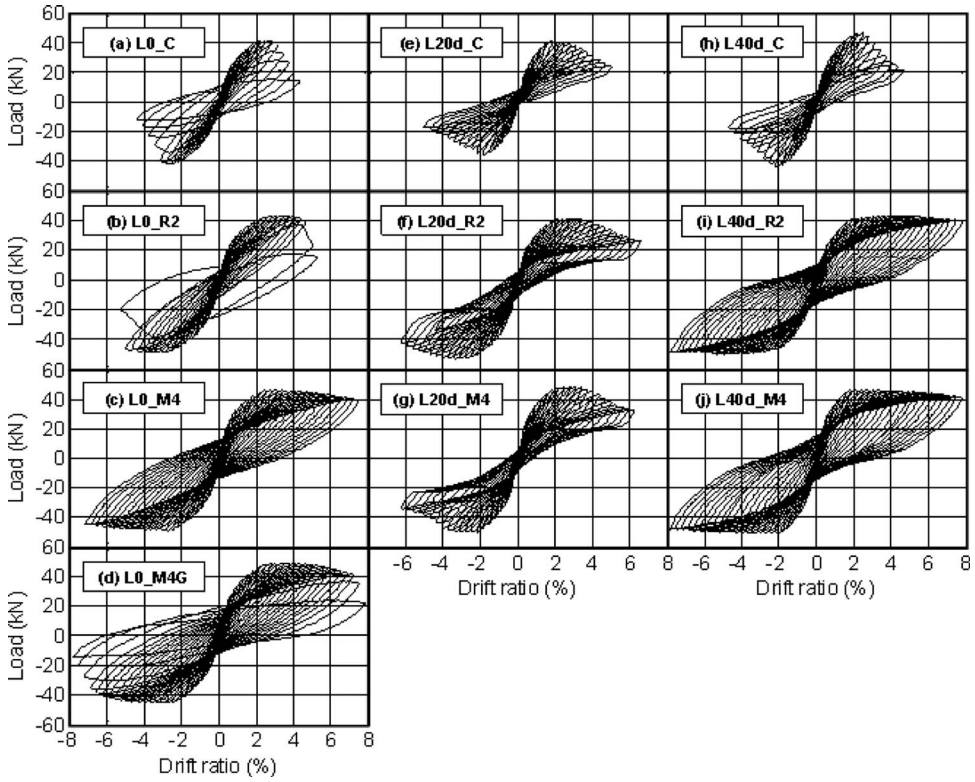

Fig. 4. Load versus drift ratio curves for all specimens tested

the column's height) loops. The corresponding envelope curves are given in Fig. 5. Key results are also presented in Table 2, which includes: (a) the peak resistance in the two directions of loading; (b) the drift ratio corresponding to peak resistance in the two directions of loading; (c) the drift ratio at conventional "failure" of the column, defined as reduction of peak resistance in a cycle below 80% of the maximum recorded resistance in that direction of loading. For some specimens (L0_M4, L40d_R2, and L40d_M4) the reduction of peak resistance when the stroke of the horizontal positioned actuator was exhausted (at a drift ratio of 7.81%) was less than 20% of the maximum recorded resistance in both directions of loading. In such cases the drift ratio at conventional failure is simply stated as $>7.81\%$. (d) The curvature ductility factor, which is defined as $\mu_\phi=\phi_u/\phi_y$, where ϕ_y and ϕ_u are the mean curvatures of the column at yield (yield of longitudinal rebars according to strain gauges readings) and at failure, respectively. Note that for those specimens where the actuator's stroke was exhausted before conventional failure, ϕ_u was calculated at the end of the test. The curvature was derived from the relative rotation measured over the lower 130 mm of the column above the base, including the column section at the face of the footing and the effect of bar pull-out from the base. More specifically, the curvature was calculated by dividing the rotation θ_1 of the cross section at $\ell_1=130$ mm (calculated by dividing the sum of displacements recorded by the two transducers at opposite sides with their horizontal distance) with the distance of this section from the column base (130 mm). (e) The observed failure mode.

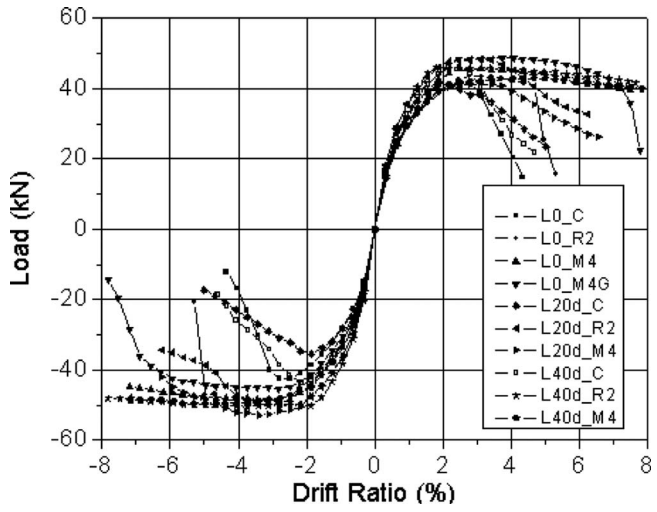

Fig. 5. Load versus drift ratio envelope curves

Specimens with Continuous Longitudinal Reinforcement

The performance and failure mode of all tested specimens with continuous longitudinal reinforcement was controlled by flexure. Buckling of longitudinal bars initiated thereupon their yielding (next loading cycle) for each specimen. The failure mode of the unretrofitted specimen was controlled by buckling of longitudinal rebars above the column base, which led to strength degradation. The outward bending of buckled bars at the column's corners (at midheight between the two adjacent stirrups closest to the column base) was found to be responsible for the concrete cover spalling over the lower 200 mm of the column [Fig. 6(a)]. The drift ratio at failure sustained by the unretrofitted column was 3.43% and the mean compressive strain (in both directions of loading) at the onset of bar buckling according to the readings of strain gauges

Table 2. Summary of Test Results

Specimen notation	Peak force (kN)		Drift at peak force (%)		Drift at "failure" (%)		Curvature ductility factor $\mu_\phi=\phi_u/\phi_y$	Failure mode
	Push	Pull	Push	Pull	Push	Pull		
L0_C	41.63	−42.48	2.5	2.5	3.43	3.43	3.84	Buckling of longitudinal bars
L0_R2	43.46	−48.70	2.8	3.1	5.0	−5.31	N/A	Buckling of longitudinal bars above FRP jacket
L0_M4	45.77	−49.19	2.8	2.8	>7.81	>7.81	14.07[a]	Conventional failure was not reached
L0_M4G	48.82	−45.28	4.0	2.8	7.5	6.9	13.22	Fracture of the TRM jacket due to both rebars buckling and concrete dilation
L20d_C	41.50	−36.62	1.87	1.87	4.06	3.12	3.54[b]	Splitting bond failure followed by spalling of the concrete cover
L20d_R2	41.26	−52.86	2.81	3.12	5.31	6.25	8.47	Splitting longitudinal cracking followed by pull-out bond failure of lapped bars
L20d_M4	48.46	−49.80	3.12	2.18	5.0	5.0	8.85	Splitting longitudinal cracking followed by pull-out bond failure of lapped bars
L40d_C	46.26	−43.82	2.5	2.18	3.43	3.12	3.10	Splitting bond failure followed by spalling of the concrete cover
L40d_R2	42.97	−49.93	4.68	5.0	>7.81	>7.81	12.20[a]	Conventional failure was not reached
L40d_M4	45.90	−50.48	1.87	3.75	>7.81	>7.81	13.01[a]	Conventional failure was not reached

[a]Curvature reached at the end of the test without conventional failure.

[b]No yielding of longitudinal reinforcement, ϕ_y calculated at peak load.

was approximately 0.70%. Typical strain histories of longitudinal column reinforcement, at the location where buckling was expected to occur, are illustrated in Fig. 7.

The behavior and failure mode of retrofitted columns (L0_R2, L0_M4, and L0_M4G) was not controlled by longitudinal bar buckling above the column base. According to measurements of strain gauges (Fig. 7) placed on longitudinal bars inside the jackets, it was observed that bar buckling was not averted for FRP or TRM confined specimens; it developed with a significant delay, ranging from 3–7 cycles with respect to their unretrofitted counterpart (L0_C), without lateral strength degradation. This is attributed to the behavior of buckled bars under external confinement. These bars could sustain a significant part of their compressive load after buckling as the concrete cover spalling remained in place and provided lateral support.

The confinement provided by the FRP jacket to Specimen L0_R2 restrained the outward bending of longitudinal bars inside the FRP jacket region. Owing to this fact the concrete cover dilation was marginal and a large amount of strain energy was stored in the confined concrete without any stress relaxation in the compression zone. This resulted in the transition of the compressive force above the FRP jacket, where buckling of longitudinal bars finally occurred abruptly in the space between the FRP jacket's end and the next stirrup at a height of 530 mm [Fig. 6(b)]. Similar observations of bar buckling above the FRP jacket (in regions with significant lower bending moment than that of the column base) have been made by other researchers too (e.g., Bousias et al. 2007).

Contrary to Specimen L0_R2, rebar buckling in Column L0_M4 and Column L0_M4G developed gradually inside the TRM-jacketed area, as the compressive force released from early buckled bars was carried by the surrounded confined concrete inside the jackets. This is possible to occur in this confining system, as TRM jackets are able to deform outwards without early

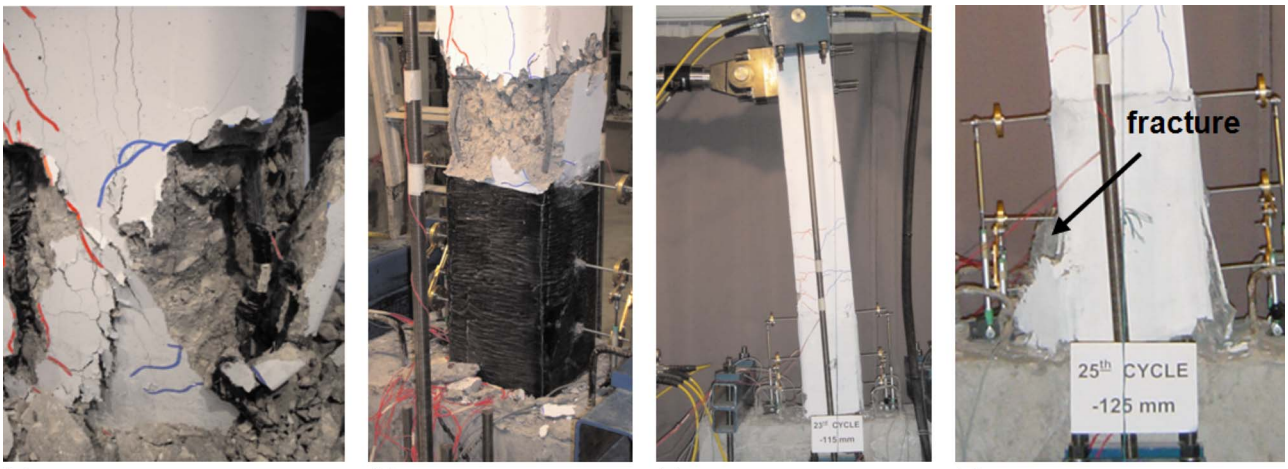

Fig. 6. (a) Disintegration of concrete and bar buckling; (b) buckling of longitudinal bars above the FRP jacket; (c) undamaged carbon TRM jacket at end of test; and (d) fracture of glass TRM jacket due to bar buckling

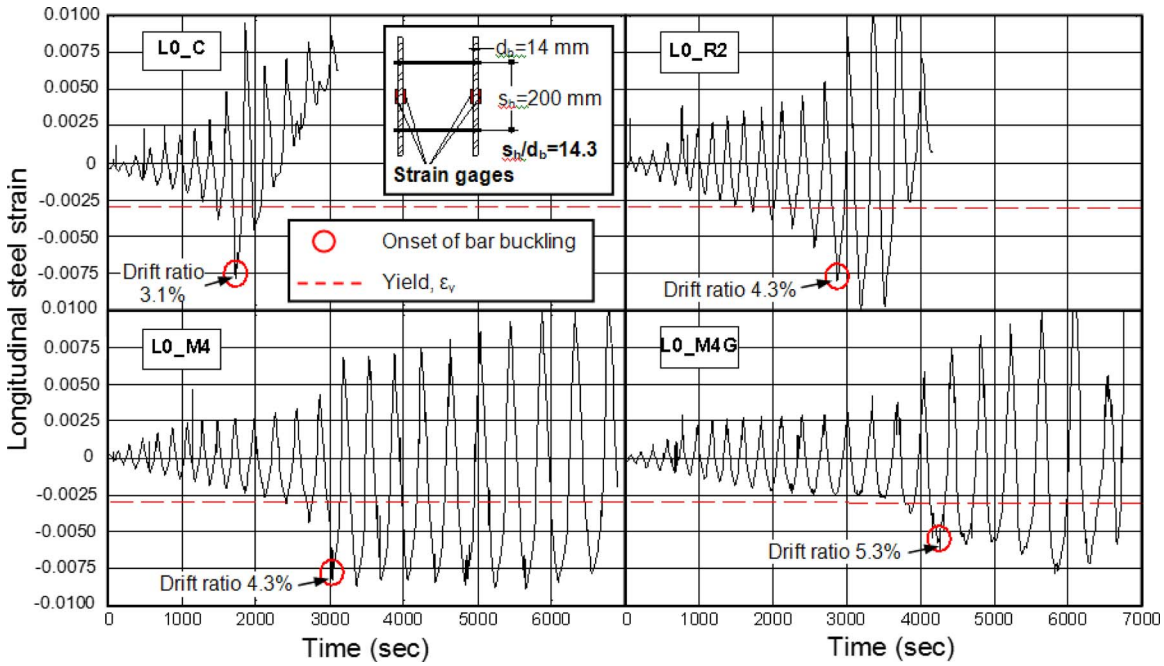

Fig. 7. Typical strain histories of longitudinal bars located at columns' base between successive stirrups

fiber rupture, due to the low composite action between fibers and mortar, which allows for higher local deformations (e.g., slip of fibers within rovings).

In Specimen L0_M4 the carbon fiber TRM jacket remained intact until the test was terminated at drift ratio equal to 7.81% [Fig. 6(c)], while in Specimen L0_M4G fracture of the glass fiber TRM jacket (at a drift ratio equal to 7.2%) led to failure [Fig. 6(d)]. Fracture of the jacket initiated from a limited number of fiber bundles when the hoop stresses reached their tensile capacity, and then propagated rather slowly in the neighboring bundles, as a result of concrete dilation and outward bending of the longitudinal rebars a little below the jacket's midheight; as a result of this gradual fiber fracture, the respective failure mode was ductile.

Overall, the behavior of carbon and glass TRM jacketed specimens was very similar, but quite different from and far better than that of the FRP confined and unretrofitted specimens. Member deformation capacity increased by a factor of 1.5, 2.3, and 2.1 for specimens L0_R2, L0_M4, and L0_M4G, respectively, in comparison with the control specimen, corresponding to drift ratios at failure equal to 5.15, 7.81, and 7.2%; this indicates a higher effectiveness of TRM versus FRP jackets, by about 50%. Peak resistance was practically the same for all jacketed specimens and about 10% higher than that of the control specimen, which experienced bar buckling at earlier stages of deformation.

Specimens with Lap-Spliced Longitudinal Reinforcement

The performance and failure mode of all specimens with lap splices was also controlled by flexure. Significant longitudinal and horizontal splitting cracks were developed along the splice length of lapped bars for both unretrofitted Specimen L20d_C [Fig. 8(a)] and Specimen L40d_C [Fig. 8(b)] at drift ratios of 1.56 and 2.5%, respectively, corresponding to peak lateral load. The length and width of the longitudinal cracks along the splice length was increasing at higher drift levels as the bond between reinforc-

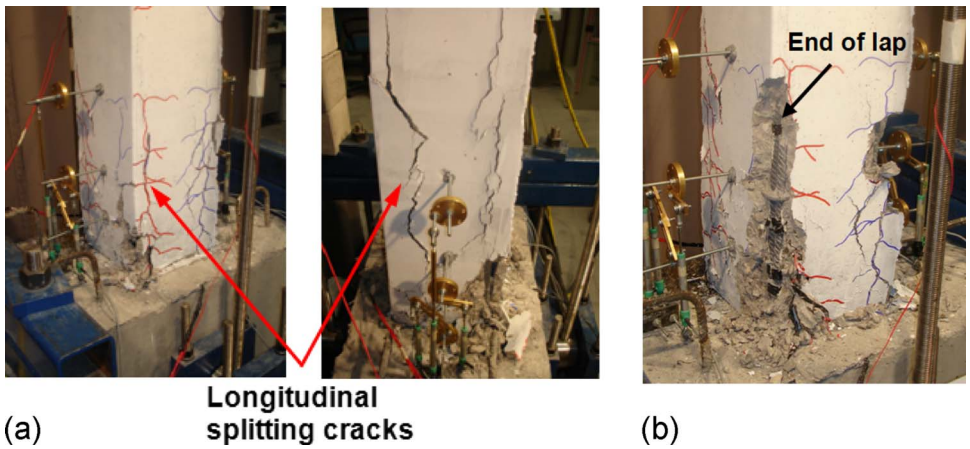

Fig. 8. Longitudinal splitting cracks for specimens (a) L20d_C; (b) L40d_C; and (c) Failure of unretrofitted Column L20d_C

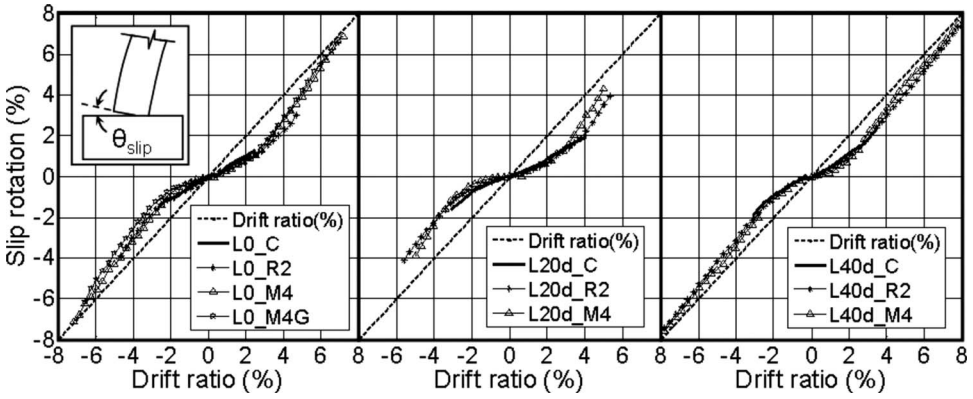

Fig. 9. Slip rotation at base in terms of drift ratio for specimens: (a) without lap splices; (b) with short lap splices; and (c) with long lap splices

ing bars and concrete was deteriorating. As a consequence of this, the concrete under compression spalled [Fig. 8(c)] along the lower (approximately) 100 and 175 mm from the base of Specimen L20d_C and Specimen L40d_C, respectively, leading to substantial lateral strength degradation after peak lateral load. Contrary to control Specimen L0_C with continuous bars, the expansive spalling of the concrete in the critical zone was not followed by buckling of longitudinal rebars for two reasons: first, the compression reinforcement was doubled; and second, the quick strength degradation of the specimens associated with the extensive bond deterioration reduced the demand of the compression reinforcement to resist the applied load. The drift ratio at failure (average values for both loading directions) sustained by unretrofitted Column L20d_C and Column L40d_C was 3.59 and 3.28%, respectively. The corresponding values for the bond strength (τ) between spliced bars and the surrounded concrete were 4.4 and 2.5 MPa. The latter was established according to the discrete strain readings along the splice length (detailed calculation of the bond stress distribution along the lap splice are given in Bournas 2008).

TRM and FRP jacketed columns, with either short or long lap length, responded far better than their unretrofitted counterparts both in terms of strength and deformation capacity at failure. Confinement provided to the columns sufficient resistance against splitting cracks and lateral expansion of concrete. Thus spalling of the concrete cover was controlled and the slip along the splice length was progressively increased in proportion to the horizontal displacement without significant bond stress deterioration.

The effectiveness of confinement was lower in the case of short lap length equal to 20 bar diameters in comparison with that of the long lap length equal to 40 bar diameters for both TRM and FRP confining systems. Specimen L20d_R2 and Specimen L20d_M4 (with short lap lengths) sustained reversed deformation cycles up to 6.3% drift before failing due to pull-out bond failure of the spliced bars at an average bond strength (in both directions of loading) between lap-spliced bars and concrete of 6.8 and 6.4 MPa, respectively. Pull-out bond failure occurred when longitudinal splitting cracks had propagated along the entire splice length; thus at that point the presence of TRM or FRP jacket had no effect on the residual splice capacity. Contrary to specimens with short lap splices, in Specimen L40d_R2 and Specimen L40d_M4 where the calculated bond stresses were much lower, namely, 3.1 and 2.9 MPa, respectively, bond failures and spalling of concrete were suppressed until the end of the test at a drift ratio of 7.81%.

For Column L20d_R2 and Column L20d_M4 the mean strength increase (in both directions of loading) for both confining systems was 20.3 and 25.6%, respectively, in comparison with the control specimen (L20d_C), while the corresponding increase in deformation capacity was 64.7 and 38.8%, respectively. Columns with longer lap splices (L40d_R2 and L40d_M4) behaved in an identical manner until the end of the test at a drift ratio of 7.81% (maximum stroke of piston was reached), resulting in an increase of the members' deformation capacity by a factor of more than 2.5. Peak resistance was practically the same as in the unretrofitted column, indicating that a lap splice length of 40 diameters is adequate for the development of the columns' full strength. Overall, it may be concluded that TRM confining jackets provide substantial gain in lateral strength and deformation capacity of cyclically loaded RC rectangular columns with lap splices at the columns' base. Compared with equal stiffness and strength FRP jackets, they are characterized by a slightly reduced effectiveness in terms of deformation capacity for columns with short lap splices and with the same effectiveness for columns with longer lap lengths.

Fig. 9 gives the relation between the drift ratio and the slip rotation θ_{slip} of the cross section at the interface between the column and the base. The latter was measured using the data from displacement transducers in two cross sections at distance $\ell_1 = 130$ and $\ell_2 = 260$ mm from the base as follows: $\theta_{slip} = \theta_2 - \phi\ell_2 = \theta_1 - \phi\ell_1$, where ϕ is the mean curvature at the column base, equals to $(\theta_2 - \theta_1)/(\ell_2 - \ell_1)$. This assumption of constant mean curvature is applicable if this distance $\ell_2 - \ell_1$ is small, in the order of: the typical distance of two adjacent flexural cracks, if the behavior prior to yielding is of interest, or the length within which concrete is expected to spall or crush and reinforcing bars may buckle or even break. In experiments, values of $\ell_2 - \ell_1$ in the range of $h/2$ to h are commonly selected. In this way it is possible to estimate the contribution of the slip rotation to the overall column deformation. The θ_{slip}-drift ratio relation is nearly bilinear for the retrofitted columns, with a first branch up to approximately the peak lateral load and a second one with higher slope from peak lateral load to conventional failure. The contribution of slip rotation to the columns overall behavior was prevalent as it comprised the major part of their deformation capacity (drift ratio). More specifically, for specimens with continuous bars the slip rotation comprised about 50, 75, and 95% of the total drift ratio of Specimen L0_C, Specimen L0_R2, and Specimen L0_M4 (and L0_M4G), respectively. For columns with lap-spliced bars, the slip rotation comprised almost 50 and 80% (short lap lengths) and 65 and 95% (long lap lengths) of the total drift ratio for unretrofitted and retrofitted specimens, respectively. Note here that the

Table 3. Energy Dissipation at Various Drift Ratios and at Failure

Specimen notation	Energy dissipated (kN/mm) and percent difference with control specimens					
	Drift 1.87%	Difference (%)	Drift 3.43%	Difference (%)	Drift 7.81% and/or failure	E_i/E
L0_C	2,176	0.0	6,219	0.0	9,870	1.0
L0_R2	2,368	8.8	7,593	22.1	20,845	2.11
L0_M4	2,834	30.2	8,707	40.0	47,841	4.85
L0_M4G	2,301	5.7	7,678	23.5	51,546	5.22
L20d_C	1,571	0.0	5,633	0.0	6,649	1.0
L20d_R2	1,782	13.4	6,514	15.6	1,8350	2.75
L20d_M4	1,876	19.4	6,725	19.4	17,190	2.58
L40d_C	1,712	0.0	5,956	0.0	7,192	1.0
L40d_R2	1,706	−0.3	7,180	20.4	64,610	8.98
L40d_M4	2,038	19.0	8,413	41.0	72,130	10.03

slip rotation is mostly attributed to the large crack opening at the base of the columns (inset of Fig. 9), which is a function of the horizontal displacement. Therefore the slip rotation was larger for columns which sustained larger drift ratios before conventional failure irrespective of the presence of lap splices bars or their length.

Stiffness and Energy Dissipation

To evaluate further the effectiveness of TRM versus FRP jacketing, the stiffness, and cumulative dissipated energies—computed by summing up the area enclosed within the load versus piston displacement curves—were recorded for each loading cycle. The dissipated energy for each specimen is provided for drift ratio levels of 1.87 and 3.43% and at the specimen's conventional failure in Table 3 and during testing in Fig. 10(a). For specimens with continuous longitudinal reinforcement, the energy dissipated at conventional failure by the TRM jacketed columns (L0_M4 and L0_M4G) was about five times higher than that dissipated by the unretrofitted column (L0_C) and about 2.5 times higher than the energy dissipated by the FRP jacketed column (L0_R2). On the other hand, the energy dissipation capacity of the two retrofitting schemes (TRM versus FRP), for the specimens with lap splices, was about the same regardless of the lap length. In particular for Series L20d_… the energy dissipated by the retrofitted columns was about 2.5 times higher than that dissipated by the unretrofitted column, while for Series L40d_…, where confinement was much more effective, the corresponding value was approximately 9. Finally, the comparison of the stiffness versus drift ratio shown in Fig. 10(b) illustrates that the stiffness reduction beyond peak load was similar for both retrofitting schemes and considerably lower in comparison with that of the unretrofitted specimens.

Comparison of Test Results with Code Formulations

The cyclic deformation capacity of RC columns, a key property in displacement-based design used in seismic rehabilitation applications, is typically expressed through the members' attained drift ratio at failure. This important parameter for all specimens tested is compared in this section with predictions given by Eurocode 8 EN 1998-3 (European Committee for Standardization 2005). The drift ratio, which is defined as chord rotation capacity at ultimate in Eurocode 8, is given by the following empirical expression:

$$\theta_u = k0.016(0.3^{\nu})\left[\frac{\max(0.01,\omega')}{\max(0.01,\omega)}f_c\right]^{0.225}\left(\frac{L_V}{h}\right)^{0.35}25^{c}(1.25^{100\rho_d}) \quad (1)$$

where f_c=compressive strength of concrete (MPa); ω and ω' =mechanical reinforcement ratio of tension and compression longitudinal reinforcement, respectively; $\nu=N/bhf_c$=normalized axial force (compression taken as positive); b=width of compression zone; h=cross section side parallel to the loading direction; $L_V=M/V$=ratio of moment/shear at the end section; $c=\alpha\rho_{sx}f_{yw}/f_c$; $\rho_{sx}=A_{sw}/bs_h$=transverse steel ratio parallel to the direction x of loading; f_{yw}=yield stress of stirrups; s_h=spacing of stirrups; A_{sw}=area of transverse steel reinforcement parallel to the

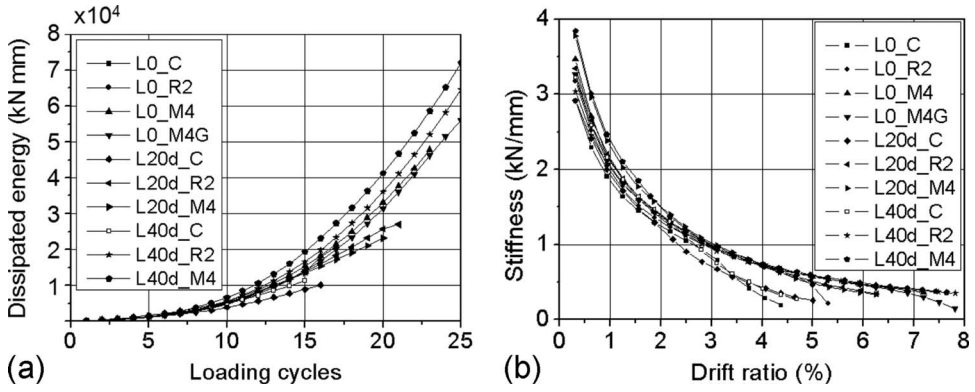

Fig. 10. (a) Cumulative dissipated energy during test; (b) stiffness versus drift ratio

direction x within s_h; k=0.825 for columns with deformed bars, without detailing for earthquake resistance; ρ_d=geometric ratio of diagonal reinforcement, if any; and α=effectiveness coefficient for confinement with stirrups.

If a column is retrofitted with an FRP or TRM jacket in the plastic hinge region, it is logical: (a) to take k equalling to 1 instead of 0.825, as the lack of detailing for earthquake resistance has been compensated by the external confinement; and (b) to adopt the expression in Eq. (1) with c given by the sum of two terms—one to account for the contribution of stirrups and a second one to account for the contribution of the jacket, as follows (Bournas et al. 2007):

$$c = a\rho_{sx}\frac{f_{yw}}{f_c} + a_f\rho_{fx}\frac{f_{fe}}{f_c} \tag{2}$$

where $\rho_{fx}=2nt_f/b$; n=number of layers of the fiber sheet or textile; t_f=thickness of one fiber sheet or textile layer; f_{fe} =effective stress of jacket at conventional failure of the column; and α_f=effectiveness coefficient for confinement with fibers (TRM or FRP jackets), equal to

$$\alpha_f = \beta\left[1 - \frac{(b-2R)^2 + (h-2R)^2}{3bh}\right] \tag{3}$$

where R=radius at corners of the cross section. The coefficient β in Eq. (3) accounts for the reduced or enhanced effectiveness of TRM versus FRP jackets in terms of ultimate strain. On the basis of concentric compression tests on reinforced concrete prisms presented in Bournas et al. (2007), this value is about 0.9. But if jacket failure has not been reached at conventional failure of the column, no reduction (nor enhancement) should be made and β should be taken as equal to 1. It should be noted here that in view of the relatively limited experimental database on TRM jacket failures, this value of β should be taken with care. Other materials (e.g., different mortars) may result in different values for the effectiveness of TRM versus FRP. Therefore for such novel materials much more experimental work is needed to propose design values of β.

For columns in which their deformed longitudinal bars have straight ends lapped at the end section of the member, the plastic part of the chord rotation in Eurocode 8 is given by an empirical expression equivalent to Eq. (1), which should be applied with the value of compression reinforcement doubled, as follows:

$$\theta_u^{pl} = k0.0145(0.25^{\nu}) \times \left[\frac{\max(0.01, 2\omega')}{\max(0.01, \omega)}\right]^{0.3} f_c^{0.2}\left(\frac{L_V}{h}\right)^{0.35} 25^c(1.25^{100\rho_d}) \tag{4}$$

If the available lap length ℓ_{ou} is less than a value of $\ell_{ou,\min}$, the plastic part of the chord rotation capacity given by Eq. (4) should be multiplied by $\ell_{ou}/\ell_{ou,\min}$

$$\ell_{ou,\min} = \frac{d_{bL}f_{yL}}{(1.05 + 14.5\alpha_l\rho_{sx}f_{yw}/f_c)\sqrt{f_c}} \tag{5}$$

where d_{bL}=longitudinal bars diameter; f_{yL}=yield stress of longitudinal bars; $a_l=a(n_{\text{restr}}/n_{\text{tot}})$; n_{restr}=number of lapped longitudinal bars restrained by a stirrup corner or a cross tie; and n_{tot} =total number of lapped longitudinal bars along the cross section perimeter. For members confined with FRP or TRM, the writers' point of view, also in agreement with Biskinis (2007), is that a_l should be replaced by a term $a_{l,f}=a_f(4/n_{\text{tot}})$, contrary to the Eurocode 8 formulation $a_{l,f}=(4/n_{\text{tot}})$, as the mechanism of confinement is the same for stirrups and composite jackets and the effectiveness coefficient must be also considered in FRP or TRM jacketed members.

Table 4. Comparison between Eurocode 8-Based Predictions and Experimentally Measured Drift Ratios at Failure

Specimen notation	Experimental drift ratio at "failure" (%)	Predicted drift ratio at "failure" (%)	Predicted/ experimental
L0_C	3.43	3.91	1.14
L0_R2	5.15[a]	7.51	1.45
L0_M4	7.81	7.79	0.99
L0_M4G	7.2	5.73	0.80
L20d_C	3.59	2.62	0.73
L20d_R2	5.78	5.51	0.95
L20d_M4	5.0	5.59	1.12
L40d_C	3.28	4.66	1.42
L40d_R2	7.81 (stroke end)	6.02	No failure
L40d_M4	7.81 (stroke end)	6.02	No failure

[a]Controlled by failure at the unconfined length, outside the jacket

The value of the chord rotation at yielding θ_y added to the plastic part to obtain the total chord rotation capacity can be estimated from the following expression proposed in Eurocode 8:

$$\theta_y = \phi_y\frac{L_V}{3} + 0.0013\left(1 + 1.5\frac{h}{L_V}\right) + 0.13\phi_y\frac{d_bf_{yL}}{\sqrt{f_c}} \tag{6}$$

where the yield curvature ϕ_y can be predicted empirically according to Biskinis (2007), as $\phi_y=1.55f_{yL}/E_sd$. Eq. (6), initially derived for the calculation of θ_y for columns with continuous bars, is also applicable to columns with lap splices, with the yield moment and the yield curvature ϕ_y computed with a compression reinforcement doubled over the value applying outside the lap splice. If the straight lap length ℓ_o is less than $\ell_{oy,\min}$ $=0.3d_{bL}f_{yL}/\sqrt{f_c}$, then, M_y and θ_y should be calculated with yield stress f_y multiplied by $\ell_o/\ell_{oy,\min}$; the second term of Eq. (6) should be multiplied by the ratio of the value of yield moment M_y as modified to account for the lap splicing, to the yield moment outside the lap splice.

For the geometric and material properties of the columns with either continuous bars or with lap splices tested in this study, the predicted and experimentally measured drift ratios at failure are presented and compared in Table 4 for all retrofitted and unretrofitted specimens. For columns with continuous bars the predicted drift ratios at failure according to the Eurocode 8—based approach described above are 14% higher than the experimental value for the unretrofitted specimen (L0_C) and 20% lower than the experimental value for the specimen retrofitted with glass fiber TRM jacket (L0_M4G). For specimen L0_M4 the predicted drift ratio is practically equal to the experimental one, but the latter was determined at the end of the test (the reduction of resistance was equal to 12% of the maximum recorded resistance) and not at conventionally defined failure. No comparison can be made for Specimen L0_R2 as its deformation capacity was controlled by the unconfined length above the FRP jacket. It can be concluded that the Eurocode 8-based formulation, as modified here, is in moderate to good agreement for members with continuous deformed bars jacketed with TRM or FRP. Finally, for columns with deformed lap-spliced bars the Eurocode 8 predicted drift ratios (with the modified value for $a_{l,f}$) are in quite good agreement for FRP and TRM jacketed members with shorter lap lengths. This is not the case in columns with longer lap splices, where the Eurocode 8-based formulation presented above was

found to be quite conservative, as the 6.02% predicted drift is far from the ultimate drift at failure. Note here that when the test was terminated at a drift ratio of 7.81% the average reduction of resistance for Specimen L40d_R2 and Specimen L40d_M4 was only 6% of the maximum resistance.

Conclusions

The effectiveness of TRM jackets as a means of confining RC columns with limited capacity due to buckling of the longitudinal bars or due to bond failure at lap splice regions is investigated in this study. Comparisons with equal stiffness and strength FRP jackets allows for the evaluation of the effectiveness of TRM versus FRP. The 10 tests on full scale columns under cyclic uniaxial flexure show that TRM jackets are quite effective as a means of increasing the cyclic deformation capacity and the energy dissipation of oldtype RC columns with poor detailing, by delaying bar buckling or by preventing splitting bond failures at columns with inadequate lap splices. More specific conclusions are summarized in a rather qualitative manner as follows:

- The four tests on columns with continuous longitudinal reinforcement (Series L0_…) show that TRM jackets are quite effective as a means of increasing the cyclic deformation capacity and the energy dissipation of oldtype RC columns with poor detailing, by delaying bar buckling. Compared with equal stiffness and strength FRP, TRM jacketing has a higher effectiveness by about 50%.
- From the six tests on columns with lap-spliced longitudinal reinforcement (Series L20_… and Series L40d_…), it may be concluded that TRM confining jackets provide substantial gain in lateral strength and deformation capacity of cyclically loaded reinforced concrete columns with lap splices at the columns' base. Compared with equal stiffness and strength FRP jackets, they are characterized by a slightly reduced effectiveness in terms of deformation capacity for columns with short lap splices and with the same effectiveness for columns with longer lap lengths.
- The Eurocode 8-based modified formulation is in moderate to good agreement for members with continuous deformed bars jacketed with TRM or FRP. For columns with deformed lap-spliced bars the Eurocode 8 predicted drift ratios are in good agreement for FRP and TRM jacketed members with shorter lap lengths, while its predictions are quite conservative in the case of columns with longer lap splices.

Despite their relatively limited number, all test results presented in this study indicate that TRM jacketing is an extremely promising solution with great potential for the confinement of poorly detailed reinforced concrete columns in seismic regions. Hence future research should be directed toward providing a better understanding of parameters including the level of axial load, initial column damage, different shear spans, different loading histories, other cross sections, and the effectiveness of TRM versus FRP for seismic retrofitting after fire exposure.

Acknowledgments

The writers thank Lecturer C. Papanicolaou, for her assistance in the experimental program. The work reported in this paper was funded by the Greek General Secretariat for Research and Technology through the project ARISTION, within the framework of the program "Built Environment and Management of Seismic Risk."

Notation

The following symbols are used in this paper:

A_{sw} = area of transverse steel reinforcement parallel to the direction x within s_h;
b = cross section width, width of compression zone;
c = coefficient;
d = effective depth of cross section;
d_{bL} = diameter of lapped bars;
E_s = elastic modulus of steel;
f_c = compressive strength of concrete;
f_{fe} = effective stress of jacket at conventional failure of the column;
f_{yL} = yield stress of longitudinal reinforcement;
f_{yw} = yield stress of stirrups;
h = cross section height, side parallel to the loading direction;
k = coefficient;
L_V = ratio of moment/shear at the end section;
ℓ_i = distance of cross section i from the column base, $i=1$, 2, and 3;
ℓ_o = lap length;
ℓ_{ou} = available lap length;
$\ell_{ou,\min}$ = minimum lap length for the calculation of ultimate chord rotation;
$\ell_{oy,\min}$ = minimum lap length for the calculation of yield chord rotation;
ℓ_s = lap length;
M = moment at end section;
M_y = yield moment of cross section;
N = axial force;
n = number of layers;
n_{restr} = number of lapped bars laterally restrained by a stirrup corner or a cross-tie;
n_{tot} = total number of lapped bars along the cross section perimeter;
R = radius at corners of cross section;
s_h = spacing of stirrups;
t_f = thickness of one fiber sheet or textile layer;
V = shear at end section;
x = direction of loading;
α = effectiveness coefficient for confinement with stirrups;
α_f = effectiveness coefficient for confinement with fibers;
β = TRM versus FRP jacket confining effectiveness in terms of strength;
θ_i = rotation of cross section i, $i=1$ and 2;
θ_{slip} = slip rotation at column base;
θ_u = chord rotation (drift ratio) at ultimate;
θ_u^{pl} = plastic part of the chord rotation (drift ratio) at ultimate;
θ_y = chord rotation (drift ratio) at yielding;
μ_ϕ = curvature ductility factor;
ν = normalized axial force;
ρ_d = geometric ratio of diagonal reinforcement;
ρ_{fx} = ratio of fibers parallel to the direction x of loading;

ρ_{sx} = transverse steel ratio parallel to the direction x of loading;
ϕ = mean curvature at column base;
ϕ_u = ultimate curvature at column base;
ϕ_y = yield curvature at column base;
ω = mechanical reinforcement ratio of tension longitudinal reinforcement; and
ω' = mechanical reinforcement ratio of compression longitudinal reinforcement.

References

Biskinis, D. E. (2007). "Deformations of concrete members at yielding and ultimate." Ph.D. thesis, Civil Engineering Department, University of Patras, Patras, Greece, 528 (in Greek).

Bournas, D. A. (2008). "Strengthening and seismic retrofitting of RC columns with advanced materials: Textile reinforced mortar, near surface mounted FRP or stainless steel reinforcement." Ph.D. thesis, Civil Engineering Department, University of Patras, Patras, Greece (in Greek).

Bournas, D. A., Lontou, P. V., Papanicolaou, C. G., and Triantafillou, T. C. (2007). "Textile-reinforced mortar (TRM) versus FRP confinement in reinforced concrete columns." *ACI Struct. J.*, 104(6), 740–748.

Bousias, S. N., Spathis, A.-L., and Fardis, M. N. (2007). "Seismic retrofitting of columns with lap spliced smooth bars through FRP or concrete jackets." *J. Earthquake Eng.*, 11(5), 653–674.

Brameshuber, W., Brockmann, J., and Roessler, G. (2001). "Textile reinforced concrete for formwork elements—Investigations of structural behaviour." *FRPRCS-5 fiber reinforced plastics for reinforced concrete structures*, C. J. Burgoyne, ed., Vol. 2, T. Telford, London, 1019–1026.

Brueckner, A., Ortlepp, R., Weiland, S., and Curbach, M. (2005). "Shear strengthening with textile reinforced concrete." *Proc., 3rd Int. Conf. on Composites in Construction*, Lyon, 1307–1314.

Curbach, M., and Jesse, F. (1999). "High-performance textile-reinforced concrete." *Structural engineering international*, Vol. 4, IABSE, Zurich, 289–291.

Curbach, M., and Ortlepp, R. (2003). "Besonderheiten des Verbundverhaltens von Verstaerkungsschichten aus textilbewehrtem." *Colloquium on textile reinforced structures*, M. Curbach, ed., 2nd Ed., Dresden, 361–374 (in German).

European Committee for Standardization. (1993). "Methods of test for mortar for masonry—Part 11: Determination of flexural and compressive strength of hardened mortar." *EN 1015-11*, Brussels, Belgium.

European Committee for Standardization. (2005). "Eurocode 8: Design of structures for earthquake resistance—Part 3: Assessment and retrofitting of buildings." *EN 1998-3*, Brussels, Belgium.

Hegger, J., and Voss, S. (2007). "Application and dimensioning of textile reinforced concrete." *FRPRCS-8 fiber-reinforced polymer reinforcement for concrete structures*, T. C. Triantafillou, ed., University of Patras, Patras, Paper No. 17-3.

Triantafillou, T. C., and Papanicolaou, C. G. (2006). "Shear strengthening of reinforced concrete members with textile reinforced mortar (TRM) jackets." *Mater. Struct.*, 39(1), 85–93.

Triantafillou, T. C., Papanicolaou, C. G., Zissimopoulos, P., and Laourdekis, T. (2006). "Concrete confinement with textile-reinforced mortar jackets." *ACI Struct. J.*, 103(1), 28–37.